J. Fluid Mech. (2008), *vol.* 607, *pp.* 401–411.
doi:10.1017/S0022112008002000 Printed in the United Kingdom

Morphology of a stream flowing down an inclined plane. Part 2. Meandering

B. BIRNIR[1], K. MERTENS[2], V. PUTKARADZE[2,3] AND P. VOROBIEFF[3]

[1]Department of Mathematics, University of California, Santa Barbara, CA 93106, USA
[2]Department of Mathematics, Colorado State University, Fort Collins, CO 80235, USA
[3]Department of Mechanical Engineering, The University of New Mexico, Albuquerque, NM 87131, USA

(Received 21 December 2007 and in revised form 16 April 2008)

A stream of fluid flowing down a partially wetting inclined plane usually meanders, unless the volume flow rate is maintained at a highly constant value. Here we investigate whether the meandering of this stream is an inherent instability. In our experiment, we eliminate meandering on several partially wetting substrates by reducing perturbations entering the flow. By re-introducing controlled fluctuations, we show that they are responsible for the onset of the meandering. We derive a theoretical model for the stream shape, which includes stream dynamics and forcing by external noise. The deviation $h(x)$ from a straight linear stream $h(x)=0$ shows considerable variability as a function of downstream distance x. However, for an ensemble average of stream shapes acquired at different times, the power spectrum $S(k)$ as a function of wavenumber k has a power-law scaling $S(k) \sim k^{5/2}$. Moreover, the area $A(x)$ swept by the stream at the distance x grows as $A(x) \sim x^{1.75}$.

1. Introduction

Studies of rivulets in the laboratory are in part driven by the visual similarity between rivulet and 'real' river meanderings. Studying the latter is much harder due to the relevance of many highly complex and intertwined phenomena, which are difficult to control: turbulence in the water, soil erosion on the riverbed, variability of the soil properties, seasonal variations of the flow rate, etc. Two approaches to modelling of river meandering exist. First, there are derivations of dynamical equations based on first principles (Leopold & Wolman 1960; Ikeda, Parker & Sawai 1981); Seminara (2006) provides a thorough review. Second, there is a stochastic approach with noise simulating the effects of turbulence and landscape variations (e.g. Birnir 2007; Birnir, Hernandez & Smith 2007).

With rivers as motivation, rivulets meandering on a partially wetting surface (glass or specially fabricated plastics, e.g. Mylar or polyethylene terephthalate) have attracted much recent attention (Davis 1980; Weiland & Davis 1981; Mizumura 1993; Mizumura & Yamasaka 1997; Le Grand-Piteira, Daerr & Limat 2006). The connection to rivers, somewhat tenuous in view of many differences in the physics, is often stated explicitly in these works, for example, by Mizumura (1993). Davis (1980) and Weiland & Davis (1981) studied the stability of a rivulet with a fixed contact line, a moving contact line with a fixed contact angle, and a moving contact line with the angles dependent smoothly on velocity. They concluded that for the fixed contact line, the straight rivulet is stable if the flow is slow enough. For the moving contact

line with a fixed contact angle, the rivulet was unconditionally unstable. Finally, for the contact angle α depending smoothly on the transverse rivulet velocity v, the stability was found to depend strongly on the value of the derivative $\mathrm{d}\alpha/\mathrm{d}v$. This approach was further developed by Young & Davis (1987), who studied the effects of contact line motion and slip at the surface on the stability. Here one must make a distinction between studies focused on sinuous (meandering) instability (Nakagawa & Scott 1984; Mizumura 1993), and on varicose and kinematic-wave instability (Davis 1980; Weiland & Davis 1981; Young & Davis 1987). While varicose (capillary) instability plays an important role in droplet formation in our experiments, this paper is concerned primarily with the behaviour of sinuous instabilities. In addition, Culkin & Davis (1984) used different substrates (including acrylic) and discussed the stability/instability conditions using a model of slender rivulets with a high Reynolds number, pressure gradients generated by curvature, and surface tension and contact-angle hysteresis balance (also see Kim, Kim & Kang 2004). Experiments and to some extent theories (Nakagawa & Scott 1984; Schmuki & Laso 1990; Nakagawa 1992) hinted at a stability boundary, beyond which there was a bifurcation to an unstable regime. Such stability boundaries of different regimes, as well as various quantities in a meandering stream on different substrates (e.g. the leading unstable wavelength), were assessed by Mizumura & Yamasaka (1997) and Le Grand-Piteira *et al.* (2006). Again, the latter study deemed the contact-angle hysteresis to play a major role.

These works concentrated on the dynamical approach, treating meandering as an inherent instability of the rivulet. Further development of the theory was inhibited by the unresolved complexities of the contact-angle behaviour (see deGennes 1985 for fundamental reference). Nevertheless, by the end of 1990s it seemed that the instability of the flow for high flow rates had been established and the problem was solved at least in principle. Three major conclusions can be derived from earlier works. First, above a certain flow rate, meandering is inevitable, at least for some surfaces. Second, a dominant wavelength exists in the meandering regime. Third, a regime of stationary meandering is realized for parameter values different from the time-dependent meandering. Many of these earlier works, inasmuch as they deal with the onset of meandering, examine a flow regime different from the one we focus on here, as it will be explained later.

In a surprising (and largely unnoticed) work by Nakagawa & Nakagawa Jr (1996) on re-stabilization of the rivulets in the regimes presumed unstable, the formation of braids, or a varicose instability of the rivulet, close to the stream origin was reported (the braids were called beads of a rosary in that paper). Mertens, Putkaradze & Vorobieff (2004, 2005) observed rivulet re-stabilization for a large range of flow parameters and explained braiding theoretically, finding the transition boundary between the braiding and non-braiding regimes. The experiments described here are a continuation of this work.

First, by eliminating flow rate disturbances, we can completely suppress the meandering for all parameter values attainable in our experiment. Re-introducing the disturbances back into the stream makes the stream meander; turning off the disturbances reliably stabilizes the stream. The stabilization is achieved more easily for higher flow rates. This applies to all the substrates we used (static contact angles ranging from 57° to 99°), and to all the water/glycerin mixtures we employed (from pure water to 50/50 mixture). Second, we show that, while a large variety of meandering profiles is realized, the power spectrum of even a small data set of meandering flow fields shows a power-law behaviour and thus rules out the existence

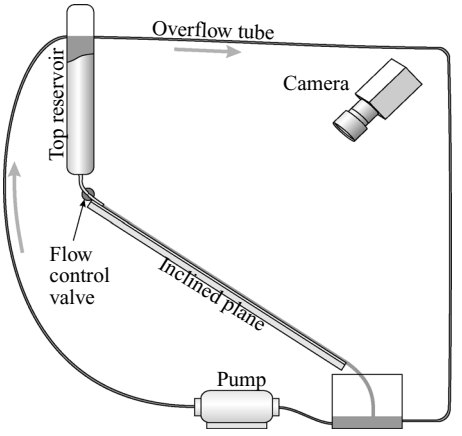

FIGURE 1. Schematic of the experimental arrangement.

of a dominant wavelength (although some leading wavelength still may characterize the onset of meandering). In a sense, meandering is akin to turbulence, where all wavelengths are present. Third, at flow rates attainable at our experiments (Reynolds number 500–18 000), we were unable to produce repeatable observations of the stationary meandering regime.

In our experiments, rivulet meandering on a partially wetting smooth surface is triggered by disturbances in the flow. Thus it is necessary to use the stochastic approach to the problem, which is the object of the theoretical part of the paper and has not been considered before. There are two stochastic forces at work here: first, the flow rate disturbances that cause the meandering; and second, the forcing of the stream by droplets left on the surface by the previous meanderings. The final results of our theory depend on the presence of these droplets, but are independent of the exact nature of their distribution in the plane, as long as this distribution remains more or less uniform downstream. With this approach, we formulate a stochastic theory explaining all the available experimental data with no fitting parameters.

The proper choice of dimensionless parameters that uniquely characterize the flow is not easy. To define the Reynolds number $R = U_* L_* / \nu$, for U_* and L_* we could use the velocity and diameter of the fluid jet contacting the incline at the source of the rivulet. This leads to $\mathrm{R} \sim 50$–400. Alternatively, we can define U_* as the terminal velocity of the straight rivulet downstream and L_* as the typical depth of this rivulet, leading to $\mathrm{R} \sim 200$–5000, Finally, we could also define L_* as the width of the rivulet, leading to $\mathrm{R} \sim 500$–18 000. The Froude number is defined with less ambiguity as $F = g \cos\alpha H_* / U_*^2$ for velocity U_* and depth H_* far downstream: $\mathrm{F} \sim 0.1$–10.

2. Experimental setup and observations

The experimental arrangement (figure 1) provides a highly constant discharge rate from a very tall cylindrical (2 m) top reservoir through a hole in its bottom connected to a flexible plastic tube. The diameter of this tube, and the hole, is $d = 3$ mm. The diameter of the container is $D = 15$ cm. Thus $d \ll D$, and the flow discharge rate Q is well approximated by the formula originally introduced by Torricelli (Clanet 2000), $Q = \pi d^4 / (4D^2)\sqrt{2gZ}$, where g is acceleration due to gravity and Z is the height differential between the location of the hole and the free surface. Thus, if Z

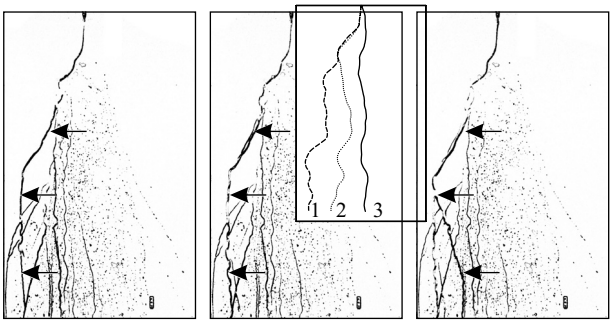

FIGURE 2. Time sequence of images (left to right) showing meandering flow. The images are processed with an edge-detection filter that emphasizes droplets deposited on the surface and makes it possible to observe both the current and the former rivulet paths. Arrows denote the current flow path. Interval between images is 7.5 s. Inset shows similar behaviour of simulated meandering flow.

remains constant, $Q \equiv$ const as well. For a fixed tube diameter, Q can be altered by changing Z.

The flow is carried to the incline by a flexible tube, necessary to prevent any capillary instabilities forming on the free surface of the water jet. An electrically driven valve can alter the flow rate by squeezing the tube, reducing its cross-section by $\sim 20\,\%$.

The inclined plane is a large (2.4 m long and 1.2 m wide) sheet of acrylic plastic (3.2 mm thick) on top of a 2.4 m $\times$ 1.2 m $\times$ 2.5 cm polypropylene slab, which in turn is mounted on a welded–steel frame. This frame is attached to two pivots, with a screw arrangement controlling its angle of incline α with respect to the horizontal.

After the flow exits the tube, it runs down the incline and into a bottom reservoir, from which it is recirculated with an electric pump connected to the top reservoir. Note that the top and bottom reservoirs are also connected with an overflow tube, which ensures that the free surface of the top reservoir remains at a constant level.

Figure 2 shows the flow of water with trace amounts of food colouring, captured with a 4-megapixel greyscale digital camera mounted above the incline. The effective resolution of the images is about 1 mm per pixel. Any optical distortions are removed from these images as follows. An image of a rectangular grid is captured by the camera. This bitmapped image with any distortions is then mapped to the bitmap containing the undistorted image. The mapping procedure produces a bicubic spline mapping scheme which is then used to process the experimental images. Prior to each experimental run, a background image with no stream is captured, to be subtracted from the images showing the stream and the droplets left in the process of its meandering. Subsequently, the centreline of the stream is extracted from the processed images. Our conservative estimate of the cumulative error of the extraction and distortion correction for the centreline coordinates is of the order of one pixel (about 20% of the characteristic stream width). The stream of fluid in this setup is highly controllable. After some initial settling time, the stream flowing down the plane assumes a straight shape for all the flow regimes we investigated. During the settling time, three distinct flow regimes could be observed: first, a region in the immediate downstream where stabilization had occurred; second, a region of continuous meandering; and third, a region where the stream breaks up. In the third

regime, stream splitting events usually occur at the inflection points of the stream. Schmuki & Laso (1990) report that these events follow elegant scaling laws.

If the flow control valve remains open (no flow rate disturbances), the stream always stabilizes to the stationary non-meandering shape. Note that the long and narrow top reservoir stabilizing the flow is crucial for rivulet stabilization. If that reservoir is removed, or a flat and shallow reservoir is used (even having the same volume capacity), the meandering never stops owing to the inherent disturbances introduced by the pump. Thus, careful attention to disturbances in the flow is imperative for this experiment. For the same reason, we avoid intrusive flow-rate measurement devices (e.g. rotameters). Flow rates are measured by collecting the fluid at the bottom of the incline. Note also that even under ideal circumstances, the transient period before the stabilization can be quite long, depending on the length of stable flow desired.

The steady-state regime is described in our previous work, see Mertens *et al.* (2004, 2005). To destabilize the rivulet and produce continuous meandering, we added an electronically operated valve to our original flow system, introducing flow rate fluctuations at will, which destabilize the straight rivulet flow, producing meandering at all the attainable flow rates. Several valve operation cycles were used, with the valve compressing the tube for 0.1 s every 1 s, for 0.1 s every 3 s, and for 0.05 s every 0.25 s. After the preliminary investigation showed no discernible differences in the stream behaviour, the subsequent experiments were conducted with the 0.1 s contraction in every 1 s cycle.

When the valve is switched off, the stream returns to the straight shape, with long relaxation times for smaller flow rates. In a few cases when a meandering pattern became stationary without straightening out (stationary meandering, Le Grand-Piteira *et al.* 2006) this effect could always be attributed to the sedimentation of dust particles on the surface. Cleaning the surface and re-starting the experiment led to re-emergence of the non-stationary meandering if flow rate disturbances were present in the flow. Without disturbances, restarting the experiment produced a straight rivulet.

Some of the discrepancy between our findings and previous literature may be due to the difference in the surface wetting properties. It was noted by Le Grand-Piteira *et al.* (2006) that surface properties play a crucial role in this phenomenon. The presence of the droplets could explain an apparent discrepancy between our results and some earlier works, since the stream could deposit droplets in different fashions for different surfaces. Note that, for all surfaces we have used (acrylic, acrylic with hydrophobic coating, and polypropylene) the spectrum results reported in this paper are identical, although individual meandering profiles, characteristic amplitudes, as well as droplet distributions, are very different.

3. Governing equations

Consider the flow of fluid on an inclined plane at an angle α with the horizontal. Let us define the (x, y) Cartesian coordinate system in this plane so that its origin coincides with the origin of the stream, and the x-axis is pointing straight downstream (i.e. the centreline of a non-meandering rivulet will follow the x-axis). Then the momentum equation for the fluid in the rivulet can be written as

$$\frac{\mathrm{d}\boldsymbol{U}}{\mathrm{d}t} + \boldsymbol{U}\cdot\nabla\boldsymbol{U} = \frac{1}{\rho}\nabla P + g\sin\alpha\hat{\boldsymbol{e}_x} + \nu\nabla^2\boldsymbol{U} + \boldsymbol{H}, \tag{3.1}$$

where $\boldsymbol{U}$ is the fluid velocity vector, P is the pressure field, ρ the fluid density, ν its kinematic viscosity, α the angle of the incline ($\alpha = 0$ for a horizontal plane), and $\hat{\boldsymbol{e}}_x$ the unit vector pointing downstream. $\boldsymbol{H}$ denotes additional forcing, whose nature may vary depending on the specific problem. The dominant contributions to the force balance come from surface tension, friction on the bottom of the stream, and internal viscous dissipation, all of which work against fluid inertia and gravity.

We use the standard lubrication approximation to reduce the full three-dimensional equations with boundary conditions (z-axis being normal to the plane of the flow) to equations in two dimensions with z-dependence averaged out and the no-slip boundary condition implicitly accounted for, in a way similar to that described in detail in Part 1 (Mertens *et al.* 2005). The lubrication approximation is based on the assumption that the vertical velocity profile in the fluid is parabolic, owing to the non-slip boundary condition on the bottom of the stream, and the stress-free condition on the top (free surface). With these assumptions, we can show the x-component of the friction force to be $F_{f,0} = -3\nu u/l^2$, where u is the value of the x-component of velocity averaged in the z-direction and l is the average stream depth. A similar parabolic-like velocity profile is expected in the cross-stream (y) direction with velocity vanishing at the contact lines (similar to theoretical results of Perazzo & Gratton 2004). The cross-stream dependence on y over the width w can then also be averaged out. The total friction terms in this direction are then $F_{f,x} \simeq -3\nu u(1/l^2 + 1/w^2) = -\lambda u$. Thus we introduce averages of the velocity components ($\boldsymbol{U} = u\hat{\boldsymbol{e}}_x + v\hat{\boldsymbol{e}}_y$) for a given cross-section of the stream.

Let the stream discharge rate at a given location be $Q = Au$, where A is the cross-sectional area of the stream in the plane normal to the x-axis. The simplest possible form of the equation describing the free surface ζ in this plane is parabolic, $\zeta = \frac{3}{2}l(1 - 4y^2/w^2)$. The area of this section (up to a prefactor depending on the contact angle) is $A = lw$. Now, using $Q = Au = lwu$, we write the equation for the friction force as $F_{f,x} = -3\nu u^2 w\left(1 + l^2/w^2\right)/(Ql)$. The ratio w/l is related to the contact angle ϕ as follows. By evaluating $\partial\zeta/\partial y$ at $y = -w/2$ (the edge of the stream), we find its value to be $6l/w$. But this slope equals $\tan\phi$. Thus $w/l = 6/\tan\phi$ and $F_{f,x} = -18u^2(1 + (\tan\phi/6)^2)/(Q\tan\phi)$. Let $\lambda = 18\nu(1 + (\tan\phi/6)^2)/(Q\tan\phi) \simeq 18\nu/(Q\tan\phi)$. By performing a similar analysis for the y-component of the friction force, we can write the components of the friction force in the two-dimensional formulation of the problem as $F_{f,x} = -\lambda u^2$ and $F_{f,y} = -\lambda uv$.

In the pressure term, the pressure can be inferred from the influence of surface tension. Let the variation of the width of the stream $w(x,t)$ be small enough for the width to be represented by its characteristic value w. In reality, the shape of the cross-sectional area of the stream changes with time, and the contact angle is subject to hysteresis. However, if the movement of the stream is gradual (characteristic contact-line velocities associated with meandering are much lower than $\boldsymbol{U} = |\boldsymbol{U}|$), it is reasonable to assume that the variation of this shape is commensurately small, and so are the variations of w and l. For this and the subsequent derivations, we also regard the downstream velocity components as uniquely defined by the downstream distance x.

Let the deviation of the centreline of the stream from the x-axis be $h(x,t)$. For a straight rivulet, $h(x,t) \equiv 0$. Then the length of the centreline of the stream between downstream locations x_1 and x_2 is $L = \int_{x_1}^{x_2}\sqrt{1 + h_x^2}\,\mathrm{d}x$, where $h_x = \partial h/\partial x$. For a partially wetting surface with $\phi \ll 90^\circ$, the stream is shallow ($l = w\tan\phi/6$). Thus the surface area of the stream between x_1 and x_2 is roughly the same as the wetted

area $S = wL = w\int_{x_1}^{x_2}\sqrt{1+h_x^2}\mathrm{d}x$. The surface tension will tend to minimize this surface area, thus the surface tension force per unit length is $F_s = \gamma\delta S/\delta h$. Here γ is the coefficient of surface tension. Thus, the corresponding capillary force per unit volume is

$$\frac{F_s}{A} = \frac{F_s}{wl} = -\frac{\gamma}{l}\frac{\partial}{\partial x}\left(\frac{h_x}{\sqrt{1+h_x^2}}\right).$$

The component form of the equations of motion (3.1) is

$$\frac{\partial u}{\partial t} + u\frac{\partial u}{\partial x} = -\lambda u^2 + \frac{1}{A\rho}\frac{\delta S}{\delta h}\cos\theta + g\sin\alpha + \nu\frac{\partial^2 u}{\partial x^2} + \eta_x, \tag{3.2}$$

$$\frac{\partial v}{\partial t} + u\frac{\partial v}{\partial x} = -\lambda u v + \frac{1}{A\rho}\frac{\delta S}{\delta h}\sin\theta + \nu\frac{\partial^2 u}{\partial x^2} + \eta_y. \tag{3.3}$$

arise from the terms containing λ are added as the result of our use of the lubrication approximation. Angle θ in the terms representing the components of the pressure i.e. surface tension) force is the angle between the direction of the stream and the x-axis: $\tan\theta = h_x$. The components of the random force $\boldsymbol{H}$ are $\eta_x = \eta\cos\theta$ and $\eta_y = \eta\sin\theta$. We must also add the continuity equation, represented as a kinematic condition for $h(x,t)$:

$$\partial h/\partial t + u\ \ \partial h/\partial x = v. \tag{3.4}$$

The system (3.2)–(3.4) can be further simplified by considering the order of magnitude of various terms under the assumption that $v \ll u$. Then, $h_x \ll 1$ and the surface tension term linearizes as follows:

$$\frac{\delta S}{\delta h} = -\frac{h_{xx}}{\sqrt{1+h_x^2}} \simeq -h_{xx}\,. \tag{3.5}$$

An important part of the subsequent discussion is the structure of the noise term η. There are two possibilities. First, one can takeq $\eta(x,t)$ as white noise with the correlation $\langle\eta(x,t)\eta(x',t')\rangle = A\delta(x-x',t-t')$. This assumption leads to an analytical solution (in a stochastic sense) for the system (3.2)–(3.4), assuming that the friction coefficient λ in (3.2)–(3.3) vanishes. The solution (presented later) yields a 1/6 meandering exponent.

Flux Q in the model is held constant. Removing the noise term we see that (3.2), (3.3) are stable, and variations in $Q(t)$ lead to small but persistent oscillations of the flow that disappear when Q is again held constant. The noise due to droplets amplifies these small flow perturbations to the amplitude, greatly exceeding that caused directly by $Q(t)$ fluctuations. Thus in the model $Q =$ const, with flow rate fluctuations present only implicitly, as a necessary factor to trigger the larger perturbations due to spatial noise. A consistent time-resolved model of meandering onset/cessation would require detailed knowledge of transient contact angle behaviour and is beyond the scope of this paper.

However, assuming $\eta(x,t)$ to be white noise is not adequate for the explanation of experimental results; the white noise character for $\eta(x,t)$ can only be assumed if there are many droplets of random sizes distributed all over the length of the meandering stream, affecting it at all times. We believe that this assumption is correct for large-scale flows, where there is continuous random forcing on all scales. However, in our experiment at each given time instant the stream encounters only a very limited number of droplets. Thus, we use the assumption that $\eta(x,t)$ is a 'spike' appearing

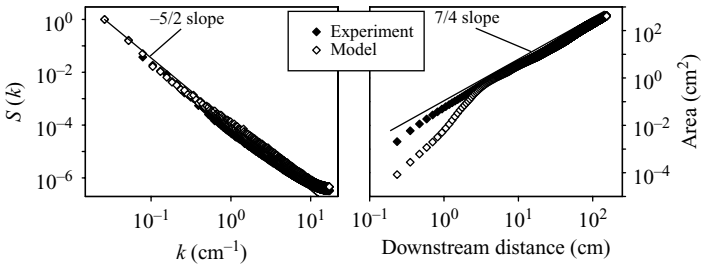

FIGURE 3. Comparison of experiments and theory (experimental data for acrylic surface). (*a*) Power spectra of the deviation of the stream from the centreline. Solid line represents $\alpha = -5/2$ power law. The noise amplitude in the model (a universal constant for all experiments) is fixed to achieve agreement at small wavenumbers k, which continues over all the k values of physical relevance. (*b*) Area between the stream and the centreline as a function of downstream distance. Solid line shows power law with exponent $7/4 = 1.75$. The deviation of the model from experiment is observed for distances comparable to the width of noise forcing, equal to the diameter of the stream.

at a random sequence of times $t_1, \ldots t_n, \ldots$. At each time t_n, the position of the spike x_n is also chosen at random. We have tried several distributions of these droplets in space, and as long as they are more or less uniform in space, the results we report below do not change for wavelengths corresponding to scales larger than droplet size. In addition, our results do not depend on the shape of each droplet as long as it is localized. We have tried a rectangular pulse function of width l, inverse Helmholtzian $\exp(-|x - x_n|/l)$ and Gaussian $\exp(-(x - x_n)^2/l^2)$. Note that in experiments, droplet size distribution changes with the substrate (Birnir *et al.* 2008), but all experimental droplet distributions on different substrates lead to the same power spectra as shown in figure 3.

Also note that all the modelling results presented here assume uniform distribution of droplet times $t_1, \ldots t_n, \ldots$; for each time t_n the distribution of droplets x_n is uniform in space. The shape of the forcing is Gaussian, with width l equal to the cross-section of the stream (2 mm). Several examples of profiles for the deviation from the centreline $h(x, t)$ are given in figure 2.

4. Quantitative analysis of experiments and comparison with theory

Our analysis is based on 105 flow images on acrylic substrate (the behaviour of the flow on other partially wettable substrates is remarkably similar statistically, see Birnir *et al.* 2008). The time intervals between the pictures were random and long enough for the flow patterns to be statistically independent. From each image at time t_m, we extracted the deviation of the stream from the centreline $h_m(x)$. From members of the ensemble $h_m(x)$, $m = 1, \ldots, 105$, we computed power spectra $S_m(k)$, where wavenumber $k = 2\pi/\lambda$ corresponds to a spatial wavelength λ. While the power spectra $S_m(k)$ based on single images are rather noisy, the spectrum produced by averaging over the ensemble $S(k)$ is a smooth graph with apparent power-law scaling $S(k) \sim k^{-5/2}$ over the span of about two decades (figure 3*a*). Fitting the data with a $-5/2$ power law yields a coefficient of determination $R^2 = 0.999$ (power-law fits presented subsequently have similar R^2 values). Averaging over as few as 30 realizations from the ensemble produces a smooth graph with the same power-law exponent. Deviation from this scaling is noticeable only for $k \geqslant k_{max} \simeq 5\,\mathrm{cm}^{-1}$, corresponding to physical scales smaller than the characteristic stream width. The largest physical scale we can

acquire (and thus the smallest wavenumber) is constrained by the 2.4 m streamwise extent of our experiment. This scaling behaviour persists for all of our experiments, representing a universal characteristic of the problem of the flow down a partially wetting incline. One important conclusion from the power-law behaviour is that for continuously meandering stream profiles, no single leading wavelength is apparent. The results were repeated for three surfaces: acrylic (contact angle $57 \pm 2^\circ$) , acrylic with hydrophobic coating (contact angle $74 \pm 5^\circ$) and polypropylene (contact angle $99 \pm 4^\circ$). The results for spectra and 'basin area' (see below) for these surfaces appear indistinguishable.

To compare the experimental results with our theory presented in § 3, we performed numerical simulation of (3.2)–(3.4) over a time up to $t \sim 10\,000$ and computed an average of the spectrum for the deviation of the centreline for an ensemble $h_m(x) = h(x, t_m)$ using a sequence of time points t_m. This spectrum is also presented in figure 3(*a*). The only fitting parameter is the normalization for noise strength $\eta(x, t)$, taken as a constant for all runs. Our theory faithfully reproduces the scaling behaviour up to the largest physically relevant values of k corresponding to the droplet forcing width.

As another test of our theory, in figure 3(*b*) we plot the area between the meandering stream and its centreline as a function of downstream distance. The deviation of the model from the power law is probably due to the length scale associated with the forcing (characteristic droplet size 1–5 mm). The area grows as $x^{7/4} = x^{1.75}$ with the distance, consistent with the power law $k^{-5/2}$ of the spectrum. Surprisingly, it is the same as the growth law for a river basin versus length of the river discovered by Hack (1957), although at the large scale this law seems to cross over to the general scaling law for correlated surfaces (Montgomery & Dietrich 1992; Dodds & Rothman 2000*b*). In our case, there is clearly no basin *per se* and no side streams forming that basin. We do not plot Hack's law data for rivers here for fear of implying that our experiment is describing river basin erosion. However, the overlap of the properly scaled data for Hack's law in figure 3 with certain river data from Rigon *et al.* (1996) would be nearly perfect. Another reason to avoid comparing our data with those from rivers is the reported variation of the exponent in Hack's law with river type (Dodds & Rothman 2000*a*). Also, the areas spanned by rivulets and the basin of rivers are very different. Basins fan out from their outlet whereas the rivulets here fan out from their source. There are no side streams on our rivulets, nor multiple sources of water (like rain) in our experiments. The coincidence of the scaling exponents is nevertheless interesting.

Thus we can conclude that the behaviour of a stream meandering down an inclined plane is dominated by the effects of the stream interacting with droplets on the plane, which can be modelled by including appropriate random forcing into the equations.

It is interesting to compare the numerical results of the model with the exact analytical solution in a stochastic sense for (3.2)–(3.4). Following previous arguments, we assume that the noise is quenched, or coloured, as in turbulence. This implies that both u and v scale as the solutions of the noise-driven Navier–Stokes equation in one-dimensional turbulence, see Birnir (2007). The stochastic solution proceeds as follows. First, we assume h_t in (3.4) to be negligible compared to uh_x and v. Then $h_x = v/u$. We define second-order structure functions $s_f = \int |f(x+\ell) - f(x)|^2 \mathrm{d}x$ (as in Frisch 1995; Birnir *et al.* 2007) and assume scaling $s_h \sim \ell^{2p_h}$, $s_u \sim \ell^{2p_u}$ and $s_v \sim \ell^{2p_v}$. The powers are related as $p_h = p_v - p_u + 1$. We can disregard the lubrication friction terms in (3.2), (3.3) by setting $\lambda = 0$, and setting η to be white noise. Then, the u equation (3.2) is simply a noise-driven Burgers equation which can be solved

exactly, giving $p_u = 2/3$. On the other hand, (3.3) can be solved exactly under these assumptions using the Feynman–Kac technique as in Simon (2005), yielding $p_v = 3/4$, and from the equation for p_h we conclude that $p_h = 1/12$ and hence $s_h = 1/6$.

Sadly, in our case setting any realistic value of $\lambda > 0$ in (3.2), (3.3) destroys the scaling $s_h = 1/6$. Also, numerics show that the characteristic time for the system to evolve $s_h = 1/6$ scaling for any realistic initial conditions is so large that it can only be observed several km downstream. It is nevertheless interesting that the meandering exponent $s_h + 1 \simeq 1.16$ agrees with that of mature rivers (1.1–1.2, Maritan *et al.* 1996).

5. Conclusions and further work

Our paper elucidates the role of disturbances in the flow rate in triggering the meandering of a fluid stream, which is then sustained by the presence of droplets left behind by earlier meanderings. We derive a model that provides an accurate description of the stochastic behaviour of the stream for all choices of parameters investigated. These results show there that is underlying structure inherent to all such partially wetting flows. Interestingly, some of the results of the model fit not only our simple experiment, but also well-established results for river morphology.

We thank Professors T. Bohr and J. Krug for fruitful discussion. V.P. is grateful for the support of the Humboldt foundation and the hospitality of the Institute for Theoretical Physics, University of Cologne.

REFERENCES

Birnir, B. 2007 Turbulent rivers. *Q. Appl. Maths* (in press)

Birnir, B., Hernandez, J. & Smith, T. R. 2007 The stochastic theory of fluvial landsurfaces. *J. Nonlinear Sci.* **17**, 13–57.

Birnir, B., Mertens, K., Putkaradze, V. & Vorobieff, P. 2008 Meandering fluid streams in the presence of flow rate fluctuations. *Physical Review Letters* submitted .

Clanet, C. 2000 Clepsydrae from Galileo to Torricelli. *Phys. Fluids* **12**, 2743–2751.

Culkin, J. B. & Davis, S. H. 1984 Meandering of water rivulets. *AIChE J.* **30**, 263–267.

Davis, S. H. 1980 Moving contact lines and rivulet instabilities. Part 1. The static rivulet. *J. Fluid Mech.* **98**, 225–242.

Dodds, P. S. & Rothman, D. 2000*a* Geometry of river networks. I. Scaling, fluctuations, and deviations. *Phys. Rev* E **63**, 016115.

Dodds, P. S. & Rothman, D. 2000*b* Scaling, universality, and geomorphology. *Annu. Rev. Earth Planet. Sci.* **28**, 571610.

Frisch, U. 1995 *Turbulence*. Cambridge University Press.

deGennes, P. G. 1985 Wetting: statics and dynamics. *Rev. Mod. Phys.* **57**, 827–863.

Hack, J. 1957 Studies of longitudinal stream profiles in Virginia and Maryland. *US Geological Survey Professional Paper* 294-B.

Ikeda, S., Parker, G. & Sawai, K. 1981 Bend theory of river meanders. Part 1. Linear development. *J. Fluid Mech.* **112**, 363–377.

Kim, H.-Y., Kim, J-H. & Kang, B. H. 2004 Meandering instability of a rivulet. *J. Fluid Mech.* **498**, 245–256.

Le Grand-Piteira, N., Daerr, A. & Limat, L. 2006 Meandering rivulets on a plane: A simple balance between inertia and capillarity. *Phys. Rev. Lett* **96**, 254503.

Leopold, L. B. & Wolman, M. G. 1960 River meanders. *Bull. Geol. Soc. Am.* **71**, 769–793.

Maritan, A., Rinaldo, A., Rigon, R., Giacometti, A. & Rodriguez-Iturbe, I. 1996 Scaling laws for river networks. *Phys. Rev.* E **53**, 15101515.

Mertens, K., Putkaradze, V. & Vorobieff, P. 2004 Braiding patterns on an inclined plane. *Nature* **430**, 165.

Mertens, K., Putkaradze, V. & Vorobieff, P. 2005 Morphology of a stream flowing down an inclined plane. Part 1. Braiding. *J. Fluid Mech.* **531**, 49–58.

Mizumura, K. 1993 Meandering water rivulet. *J. Hydraul. Engng* **119**, 1205–1222.

Mizumura, K. & Yamasaka, M. 1997 Analysis of meandering water rivulets of finite amplitude. *J. Hydraul. Engng* **123**, 995–1003.

Montgomery, D. R. & Dietrich, W. E. 1992 Channel initiation and the problem of landscape scale. *Science* **255**, 826–830.

Nakagawa, T. M. S. 1992 Rivulet meanders on a smooth hydrophobic surface. *Intl J. Multiphase Flow* **18**, 455–463.

Nakagawa, T. M. S. & Nakagawa Jr, R. 1996 A novel oscillation phenomenon of the water rivulet on a smooth hydrophobic surface. *Acta Mechanica* **115**, 27–37.

Nakagawa, T. & Scott, J. C. 1984 Stream meanders on a smooth hydrophobic surface. *J. Fluid Mech.* **149**, 89–99.

Perazzo, C. & Gratton, J. 2004 Navier-Stokes solutions for parallel flow in rivulets on an inclined plane. *J. Fluid Mech.* **507**, 367–379.

Rigon, R., Rodriguez-Iturbe, I., Maritan, A., Giacometti, A., Tarboton, D. G. & Rinaldo, A. 1996 On Hack's law. *Water Resour. Res.* **32**, 3367–3374.

Schmuki, P. & Laso, M. 1990 On the stability of rivulet flow. *J. Fluid Mech.* **215**, 125–143.

Seminara, G. 2006 Meanders. *J. Fluid Mech.* **554**, 271–297.

Simon, B. 2005 *Functional Integration and Quantum Physics*, 2nd edn. AMS Chelsea Publishing.

Weiland, R. H. & Davis, S. H. 1981 Moving contact lines and rivulet instabilities. Part 2. Long waves on flat rivulets. *J. Fluid Mech* **107**, 261–280.

Young, G. W. & Davis, S. H. 1987 Rivulet instabilities. *J. Fluid Mech* **176**, 1–30.